Current Research in Immunology 2 (2021) 120–131

Contents lists available at ScienceDirect

Current Research in Immunology

journal homepage: www.sciencedirect.com/journal/current-research-in-immunology

STAT6 signaling pathway controls germinal center responses promoted after antigen targeting to conventional type 2 dendritic cells

Fernando Bandeira Sulczewski [a], Larissa Alves Martino [a], Bianca da Silva Almeida [a], Márcio Massao Yamamoto [a], Daniela Santoro Rosa [b,c], Silvia Beatriz Boscardin [a,c,*]

[a] Departamento de Parasitologia, Instituto de Ciencias Biomedicas, Universidade de Sao Paulo, Sao Paulo, Brazil
[b] Departamento de Microbiologia, Imunologia e Parasitologia, Universidade Federal de Sao Paulo, Sao Paulo, Brazil
[c] Instituto de Investigação em Imunologia (iii), INCT, Sao Paulo, Brazil

ARTICLE INFO

Keywords:
Dendritic cells
Antigen targeting
DCIR2
Germinal center
Plasma cells
T follicular helper cells
STAT6

ABSTRACT

Conventional dendritic cells (cDCs) are antigen-presenting cells specialized in naïve T cell priming. Mice splenic cDCs are classified as cDC1s and cDC2s, and their main functions have been elucidated in the last decade. While cDC1s are specialized in priming type 1 helper T cells (T_H1) and in cross presentation, cDC2s prime T follicular helper (T_{FH}) cells that stimulate germinal center (GC) formation, plasma cell differentiation and antibody production. However, less is known about the molecular mechanisms used by cDCs to prime those responses. Here, using WT and STAT6-deficient mice (STAT6 KO), we targeted a model antigen to cDC1s and cDC2s via DEC205 and DCIR2 receptors, respectively, in an attempt to study whether the STAT6 signaling pathway would modulate cDCs' ability to prime helper T cells. We show that the differentiation and maturation of cDCs, after stimulation with an adjuvant, were comparable between WT and STAT6 KO mice. Besides, our results indicate that, in STAT6 KO mice, antigen targeting to cDC2s induced reduced T_{FH} and GC responses, but did not alter plasma cells numbers and antibody titers. Thus, we conclude that the STAT6 signaling pathway modulates the immune response after antigen targeting to cDC2s via the DCIR2 receptor: while STAT6 stimulates the development of T_{FH} cells and GC formation, plasma cell differentiation occurs in a STAT6 independent manner.

1. Introduction

Conventional Dendritic cells (cDCs) link the innate and the adaptive immune systems. They play an important role in immune surveillance, as they can sense the tissue microenvironment and quickly detect sources of infection/inflammation, as well as self-antigens (Strioga et al., 2013). Once cDCs find an antigen, they can absorb, process and present the antigens to specific T cells in order to prime an appropriate adaptive immune response (Banchereau and Steinman, 1998; Steinman and Hemmi, 2006). In this way, cDCs are central players in the immune system, and understanding cDC-mediated responses is crucial to understanding immunity and tolerance. However, we still do not fully understand all signals that regulate cDC functions, especially *in vivo*.

In the last few years, many efforts have focused on understanding the biology and ontogeny of cDCs, as they vary their membrane markers across tissues and species (Amorim et al., 2016; Anderson et al., 2020; Patente et al., 2018; Yin et al., 2021). More recently, it became clear that cDCs can be classified, according to their ontogeny, into two subsets: conventional type 1 dendritic cells (cDC1s) and conventional type 2 dendritic cells (cDC2s) (Guilliams et al., 2014). cDC1s express high levels of the transcriptional factor IRF8 that is a terminal selector for cDC1 development, and are specialized in antigen cross-presentation. On the other hand, cDC2s are low for IRF8 but express high amounts of the transcriptional factor IRF4, being mainly associated with antigen presentation via MHC class II (Dudziak et al., 2007; Guilliams et al., 2016). Murine splenic cDC1s and cDC2s are classical models for studying cDC-mediated responses *in vivo*.

The spleen is a secondary lymphoid organ where cDCs prime T cells in response to blood antigens and stimulate B cells to produce antibodies (Mebius and Kraal, 2005; Yousif et al., 2021). In the murine spleen, cDCs are strategically located to capture antigens and promote different $CD4^+$ T cell responses. Splenic cDC1s are $CD11c^+CD8\alpha^+DEC205^+$ cells that, in the steady state, are localized in the T cell zone and in the rep pulp, while cDC2s are $CD11c^+CD11b^+DCIR2^+$ cells mostly restricted to the bridging channels of the marginal zone (Eisenbarth, 2019; Lewis et al., 2019; Shin et al., 2016). Under inflammatory conditions, cDC1s migrate from the red pulp to the center of the T cell zone, whereas cDC2s migrate to the

* Corresponding author. Universidade de São Paulo - Instituto de Ciências Biomédicas II Av. Prof. Lineu Prestes, 1374 - Sala 46, São Paulo - SP, 05508-000, Brazil.
E-mail address: sbboscardin@usp.br (S.B. Boscardin).

https://doi.org/10.1016/j.crimmu.2021.08.001
Received 18 April 2021; Received in revised form 5 August 2021; Accepted 23 August 2021
Available online 28 August 2021

Abbreviation

cDC	conventional dendritic cell
cDC1	conventional type 1 dendritic cell
cDC2	conventional type 2 dendritic cell
CFSE	Carboxyfluorescein succinimidyl ester
DZ	dark zone
FLT3L	FMS-like tyrosine kinase 3 ligand
GC	germinal center
GM-CSF	Granulocyte-macrophage colony-stimulating factor
IL-13	interleukin 13
IL-4	interleukin 4
IRF4	Interferon regulatory factor 4
IRF8	Interferon regulatory factor 8
LZ	light zone
OVA	ovalbumin
PD-1	Programmed cell death protein 1
Poly (I:C)	Polyinosinic:polycytidylic acid
STAT6	Signal transducer and activator of transcription 6

outer part of the T cell zone into the white pulp (Calabro et al., 2016b). In the center of the T cell zone, cDC1s cross-talk with NK cells, plasmacytoid DCs (pDCs) and T cells in order to prime T_H1 cell responses. NK- or pDC-derived type I interferons seem to mature cDC1s and prompt them to prime T_H1 cells (Ardouin et al., 2016; Bottcher et al., 2018; Longhi et al., 2009). In contrast, in the outer part of the T cell zone, located near the B cell zone, cDC2s interact with $CD4^+$ T cells and prime T_{FH} responses, that in turn support B cell responses (Calabro et al., 2016a, 2016b; Krishnaswamy et al., 2017; Shin et al., 2015, 2016; Sulczewski et al., 2020). There is evidence suggesting that B cells play an important role in the correct positioning of $CD4^+$ T cells and cDC2s in the marginal zone in an EBI2a-dependent manner (Gatto et al., 2013; Li et al., 2016; Lu et al., 2017; Yi and Cyster, 2013).

Antigen targeting to cDCs is an efficient strategy for accessing cDC1s and cDC2s directly *in vivo*, to promote specific immune responses to an antigen, and to address functions of cDCs to study their roles and their biology (Bonifaz et al., 2002, 2004; Do et al., 2010; Dudziak et al., 2007; Longhi et al., 2009; Shin et al., 2015, 2016; Trumpfheller et al., 2008). cDC2s promote $CD4^+$ T cell proliferation and prime T_{FH} cells 4 or 5 days after an antigen is targeted via the DCIR2 receptor or blood antigens are uptaken by them (Calabro et al., 2016b; Shin et al., 2015; Sulczewski et al., 2020). The primed T_{FH} cells support germinal center (GC) formation, plasma cells differentiation and, consequentially, antibody production, class and IgG subclass switches (Shin et al., 2015; Sulczewski et al., 2020). The evidence indicating that cDC2s are specialized to promote T_{FH} cell fate is also reinforced by their expression of ICOSL and OX40L, two costimulatory molecules that trigger STAT3 phosphorylation in T cells, which is required for Bcl-6 expression (Chappell et al., 2012; Shin et al., 2015; Sulczewski et al., 2020). Furthermore, cDC2s are capable of secreting soluble CD25 that reduces the availability of IL-2, an inhibitory signal for T_{FH} cell priming (Ballesteros-Tato et al., 2012; Li et al., 2016). However, many other signals may be necessary to promote these responses.

The molecular and cellular mechanisms that control the induction of T_{FH} cells and the formation of GC in cDC2-mediated responses are not yet fully understood. In fact, interactions between cDC2s and/or T and B cells are required for induction of the T_{FH} cell fate, as well as for GC initiation and expansion (Crotty, 2011). Interestingly, these interactions take place at the border of the T and B cell zones and inside GC, which are areas that may have a particular niche to support such interactions (Eisenbarth, 2019). There is evidence that IL-4/IL-13 and STAT6 (that mediates IL-4/IL-13 signaling through IL-4R and IL-13R) limit GC expansion when mice are infected with *Nippostrongylus brasiliensis*, a Th2 infection model (Kaplan et al., 1996; Minty et al., 1993; Turqueti-Neves et al., 2014). In addition, subcutaneous immunization with NP-ovalbumin reduced GC formation in mice lacking IL-4 (Gonzalez et al., 2018). We then set out to investigate whether the STAT6 signaling pathway would modulate the responses of T_{FH}, GC, and plasma cells after antigen targeting to cDCs. Here, we show that STAT6 signaling does not alter the differentiation of cDC1s and cDC2s, nor their maturation. Besides, our results also demonstrate that STAT6 signaling in cDC2s modulates not only GC but also T_{FH} expansion and, interestingly, plasma cells differentiation occurs in a STAT6-independent manner in cDC2-mediated immune responses.

2. Material and methods

2.1. Mice

Four-to 6-week-old female and male BALB/c DO11.10, BALB/c (WT) and BALB/c STAT6 KO (kindly provided by Dr. José Carlos Farias Alves Filho, Ribeirão Preto Medical School, University of São Paulo) mice were bred at the Isogenic Mouse Facility of the Parasitology Department, University of São Paulo, Brazil and maintained in pathogen free conditions with water and food *ad libitum*. This study was performed in accordance with the Brazilian National Law on animal care (11.794/2008). The Institutional Animal Care and Use Committee (IACUC) of the Institute of Biomedical Sciences of the University of São Paulo approved the experimental procedures under the protocol number 7937100118.

2.2. Chimeric mAbs

The previously described αDEC-Ovalbumin (αDEC-OVA), αDCIR2-Ovalbumin (αDCIR2-OVA) and ISO-Ovalbumin (ISO-OVA) chimeric mAbs (Boscardin et al., 2006; Hawiger et al., 2001) were produced in human embryonic kidney (HEK) 293T cells (ATCC No CRL-11268) exactly as described elsewhere (Antonialli et al., 2017). As a quality control, after purification by affinity chromatography with protein G beads, the integrity of αDEC-OVA, αDCIR2-OVA and ISO-OVA was analyzed by SDS-PAGE and their binding capacities were tested using Chinese hamster ovary (CHO) cells expressing either the mouse DEC205 or the mouse DCIR2 and primary splenic cDC1s and cDC2s, exactly as described elsewhere (Antonialli et al., 2017).

2.3. Adoptive cell transference

Ovalbumin-specific $CD4^+$ T cells were isolated from BALB/c DO11.10 mice. Briefly, the spleens of BALB/c DO11.10 mice were removed and cell suspensions were obtained as described below. The splenocytes were incubated with anti-CD3-APC.Cy7 (clone: 145.2C11), anti-CD4-PerCP (clone: RM 4–5) and anti-CD11c-PE (clone: N418), as well as green fluorescence Live/Dead (Thermo Fisher Scientific), for 30 min on ice in the dark. All antibodies were obtained from BD Biosciences. After two washes with FACS buffer (1X PBS and 2% of Fetal Bovine Serum), live $CD11c^-CD3^+CD4^+$ cells were sorted using a FACSAria™ II Cell Sorter (BD Biosciences) with more than 90% of purity. Three million DO11.10 $CD4^+$ T cells were adoptively transferred to WT or STAT6 KO mice by intravenous route 24 h before the immunization.

2.4. Immunizations and spleen cell suspensions preparation

WT or STAT6 KO mice were immunized intraperitoneally with the chimeric mAbs. Groups received 5 μg of αDEC-OVA, αDCIR2-OVA or ISO-OVA together with 50 μg of Polyinosinic:polycytidylic acid (Poly(I:C)) (Invivogen) as an adjuvant, or only Poly (I:C) as a negative control. Mice were euthanized after blood collection five days after immunization. The spleens were removed, weighted, and processed. Red blood cells were lysed with 1 mL of ACK solution (150 mM NH_3Cl, 10 mM $KHCO_3$, 0.1 mM EDTA) and splenocytes were washed twice in RPMI

1640 (Gibco) supplemented with 2% Fetal Bovine Serum (Gibco) or in FACS buffer (1X PBS and 2% Fetal Bovine Serum). Cells were counted using the Countess Automated Cell Counter (Invitrogen).

2.5. Immunophenotyping

The detection of CD80, CD86, and CD40 in cDCs and of T_{FH}, germinal center, and plasma cells was performed by flow cytometry exactly as described previously (Sulczewski et al., 2020). Splenocyte suspensions were blocked with Fc block (clone: 2.4G2, BD Biosciences) in all experiments in which cDCs were stained. After two washes in FACS buffer, the splenocytes were stained with fluorochrome-conjugated antibodies in two steps. First, anti-CD19 (clone: 1D3), anti-CD3 (clone: 145.2C11) and anti-CD49b (clone: DX5) conjugated to biotin were added. After an incubation for 30 min on ice, the cells were washed twice in FACS buffer and then incubated with anti-MHCII-Alexa fluor 700 (clone: M5/114.15.2, I-A/I-E), anti-CD11c-BV421 (clone: N418), anti-CD8α-BV786 (clone: 53–67), anti-CD11b-PE.Cy7 (clone: M1/70), anti-CD80-FITC (clone: 16-10A1), anti-CD86-APC (clone: GL1), anti-CD40-PE (clone: 1C10) and streptavidin-APC.Cy7, as well as with Aqua Live/Dead (Thermo Fisher Scientific) or with anti-DEC205-APC (clone: NLDC-145) and anti-DCIR2-PE (clone: 33D1).

To label T_{FH} cells, anti-CXCR5-biotin (clone: 2G8), anti-TCR-DO11.10-FITC (clone: KJ1-26), anti-CD19-PE.Cy7 (clone: 1D3), anti-CD3-APC.Cy7 (clone: 145.2C11), anti-CD4-PerCP (clone: RM 4–5), anti-PD-1-APC (CD279) (clone: J43) and streptavidin-PE, including Aqua Live/Dead (Thermo Fischer Scientific), were incubated with the splenocytes exactly as described previously (Sulczewski et al., 2020).

Germinal centers and plasma cells were labeled with anti-CD3-APC.Cy7 (clone: 145.2C11), anti-B220-PerCP (clone: RA3-6B2), anti-GL-7-FITC (clone: GL7), anti-CD95-PE (clone: Jo2), anti-CD138 (clone: 281–2), and Aqua Live/Dead (Thermo Fischer Scientific). GC B cells in the dark or light zones were stained with anti-CD3-APC.Cy7 (clone: 145.2C11), anti-B220-PerCP (clone: RA3-6B2), anti-GL-7-FITC (clone: GL7), anti-CD95-PE (clone: Jo2), anti-CD83-BV421 (clone: Michel-19), anti-CXCR4-PE-CF594 (clone: 2B11/CXCR4), and Aqua Live/Dead (Thermo Fischer Scientific).

All antibodies used were purchased from BD Biosciences, with exception of anti-MHCII-Alexa fluor 700 and anti-CD11b-PE.Cy7 purchased from eBioscience, and anti-TCR.DO11.10-FITC purchased from Biolegend.

One million cells were acquired in a BD LSRFortessa™ Flow Cytometer.

2.6. Intranuclear staining of Bcl-6, T-bet, and KI67

For the detection of intranuclear Bcl-6, T-bet and KI67, splenocytes were stained for viability and surface markers as previously described, and then fixed and permeabilized with the Foxp3 labeling kit (eBioscience). Anti-Bcl6-PE (clone: K112-91) and/or anti-T-bet-BV421 (Clone: O4-46) and/or KI67-BV421 (clone: B56) were added and incubated for 1 h, on ice and in the dark. Next, splenocytes were washed twice with FACS buffer and one million cells were acquired in a BD LSRFortessa™ Flow Cytometer.

2.7. Intracellular analyses of pSTAT6

Five million splenocytes were stimulated or not with 200 ng/mL of recombinant IL-4 (Immunotools) at 37 °C for 20 min. After two washes with FACS buffer, cDCs were stained as previously described, fixed and permeabilized using BD Phosflow Perm buffer III, according to the manufacturer's instructions. pSTAT6 was stained using anti-pSTAT6-Alexa flour 488 (clone: J71–773.58.11, BD Biosciences) for 1 h on ice in the dark. Splenocytes were then washed twice in FACS buffer and one million cells were acquired in a BD LSRFortessa™ Flow Cytometer.

2.8. Analysis of serum antibodies

Blood was collected from WT and STAT6 KO mice 5 days after immunization and serum was obtained and stored in −20 °C. Specific anti-Ovalbumin antibodies (anti-OVA) were analyzed by ELISA, exactly as previously described (Sulczewski et al., 2020). Commercially available purified Ovalbumin (Sigma) at a final concentration of 2 μg/mL was used to coat high binding 96-well ELISA plates (Costar). Sera were serially diluted (dilution factor = 3) starting at 1:100. Anti-mouse IgG conjugated with HRP (SouthernBiotech), anti-mouse IgM, anti-mouse IgG1, anti-mouse IgG2a, anti-mouse IgG2b, and anti-mouse IgG3 conjugated with HRP (all purchased from The Jackson ImmunoResearch Laboratory) were used to detect antigen-bound primary antibodies. Titers represent the highest serum dilution showing an OD_{490} read higher than 0.1. The endpoint titers were normalized on a log10 scale.

2.9. DO11.10 $CD4^+$ T cell proliferation in vitro

OVA-specific transgenic $CD4^+$ T cells (DO11.10 $CD4^+$ T cells) were isolated from DO11.10 mice spleens by cell sorting (as described above) and labeled with CFSE (1.25 μM, Invitrogen). cDC2s were also isolated from WT or STAT6 KO spleens by cell sorting. Briefly, the murine spleen was digested with collagenase type IV (Gibco). After digestion, a 30% BSA centrifugation gradient was performed to enrich the cDC population in the samples before isolation (Leylek et al., 2019). After centrifugation, cells were blocked using the Fc block (BD Biosciences) followed by labeling with anti-CD19 (clone: 1D3), anti-CD3 (clone: 145.2C11) and anti-CD49b (clone: DX5) conjugated to biotin. After two washes in FACS buffer, cells were stained with anti-CD11c-PE (clone: N418), anti--CD8α-APC (clone: 53–67), anti-CD11b-PE.Cy7 (clone: M1/70), streptavidin APC.Cy7 and Live/Dead-Green (Invitrogen). cDC2s were isolated using a FACSAria™ II Cell Sorter (BD Biosciences).

Isolated cDC2s were stimulated with Ovalbumin (10 μg/mL) for 30 min at 37 °C to internalize the antigen. After two washes, cDC2s were then stimulated with 100 μg/mL of Poly (I:C) for 30 min at 37 °C. After two washes, cDC2s were co-cultured with DO11.10 $CD4^+$ T cells labeled with CFSE in different proportions of DC:T cells (1:10, 1:20, 1:40 and 1:80), using a fixed concentration of 10^5 CFSE labeled DO11.10 $CD4^+$ T cells per well. After five days in culture, $CD4^+$ T cell proliferation was analyzed by dilution of CFSE dye. Percentages (%) of proliferation were normalized by subtraction of the $CFSE^{Low}$ cells of the unstimulated control.

2.10. Data acquisition, calculation of absolute cell numbers, and statistical analysis

Flow cytometry data were acquired on the BD LSRFortessa™ Flow Cytometer (BD Biosciences) and analyzed using the FlowJo software (version 9.3, Tree Star, San Carlo, CA, USA). The frequencies obtained in the analysis of the gating strategy and the counting of spleen cells were used to calculate the absolute cells' numbers. Prism 9.0 (GraphPad, CA, USA) was used for all analyzes. Regular one-way ANOVA and one-way ANOVA for repeated measures were used for multiple comparisons, followed by Tukey test. Student's t-test was used for comparisons between two groups.

3. Results

3.1. STAT6 does not influence cDCs differentiation

In an attempt to study whether STAT6 signaling pathway modulates the immune response promoted by antigen targeting to cDCs, we used BALB/c (WT) and STAT6 KO mice. We started analyzing the absolute numbers of cDC1s and cDC2s in the spleens to check whether WT and STAT6 KO mice would have similar numbers of these cells. To do this, we stained splenocytes and performed flow cytometry to identify subsets

of cDCs using the gating strategy indicated in Fig. 1A. There were no statistically significant differences in the number of splenic cDC1s and cDC2s when we compared WT and STAT6 KO mice (Fig. 1B and C). These results indicate that WT and STAT6 KO mice have similar numbers of cDCs in the spleen, suggesting that the STAT6 signaling pathway does not alter the differentiation of splenic cDCs *in vivo*.

Furthermore, we also confirmed that STAT6 KO mice did not express STAT6 by performing a phosflow assay to ensure that STAT6 was not phosphorylated. We stimulated spleen cells *in vitro* with recombinant murine IL-4, which promotes STAT6 phosphorylation, and compared the medians of fluorescence intensities (MFIs) of phosphorylated STAT6 (pSTAT6) in cDC1s and cDC2s from WT or STAT6 KO mice. As expected, the pSTAT6 MFIs were significantly higher in WT cDC1s and cDC2s that were stimulated with IL-4 when compared with unstimulated, indicating that IL-4 promotes STAT6 activation in cDC1s and cDC2s (Fig. 1D–F). On the other hand, pSTAT6 MFIs were similar in IL-4-stimulated and unstimulated cDC1s and cDC2s from STAT6 KO (Fig. 1D–F).

3.2. αDEC205-OVA and αDCIR2-OVA bind to DEC205 and DCIR2 receptors, respectively

We used chimeric monoclonal antibodies αDEC205 and αDCIR2 linked with ovalbumin (OVA) to target cDC1s and cDC2s *in vivo*, respectively. We also used an isotype control (ISO) linked with OVA, which does not bind to any DC cell receptor, as a non-targeted control. αDEC205-OVA, αDCIR2-OVA and ISO-OVA were successfully produced (Fig. S1A). Furthermore, their ability to specifically bind to the DEC205 or DCIR2 receptors was tested using transgenic CHO cells that express the mouse DEC205 (CHO-DEC205) or DCIR2 (CHO-DCIR2) receptors. Different concentrations (5; 0.5; or 0.05 μg/mL) of the chimeric mAbs

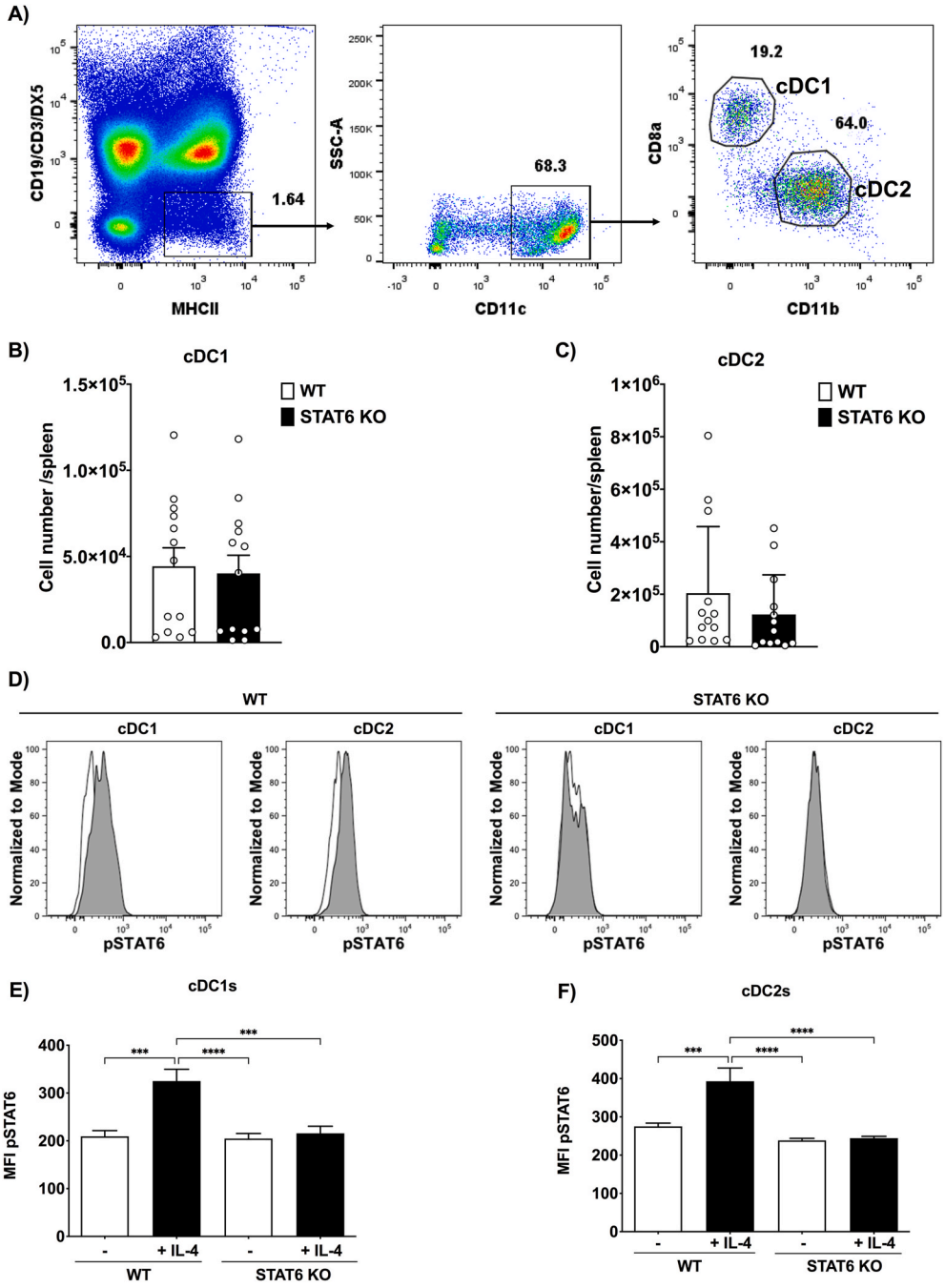

Fig. 1. cDCs subsets and STAT6 phosphorylation in STAT6-deficient mice. (A-B-C) Flow cytometry analysis of cDC1s and cDC2s from spleens of BALB/c WT and STAT6 KO mice. A) Gating strategy to identify cDC subsets. $CD19^{-}/CD3^{-}/DX5^{-}MHCII^{+}$ cells were selected and then gated on $CD11c^{+}$ cells. $CD8\alpha^{+}CD11b^{-}$ cells were considered cDC1s and $CD8\alpha^{-}CD11b^{+}$ cells were considered cDC2s. Total splenic cDC1s and cDC2s numbers were quantified according to the frequency of cDC1s (B) and cDC2s (C) cells in the flow cytometry analyses. (D-E-F) Splenocytes from BALB/c WT and STAT6 KO were stimulated or not with 200 ng/mL of recombinant murine IL-4. After blocking, spleen cells were stained, fixed and permeabilized using Phosflow Perm buffer III. Intracellular pSTAT6 was analyzed by flow cytometry in cDC1s and cDC2s. D) Histograms showing pSTAT6 in cDC1s and cDC2s from BALB/c WT or STAT6 KO mice stimulated (gray) or not (white) with IL-4. Median fluorescence intensity (MFI) for pSTAT6 was determined in cDC1s (E) and cDC2s (F). (B–C) Bars show mean ± SD of four representative experiments pooled together (n = 13 animals/group). (E–F) Bars show mean ± SD of one experiment (n = 3 animals/group). ***p < 0.001 and ****p < 0.0001; one-way ANOVA followed by Tukey's post-test.

were incubated with CHO-DEC205 or CHO-DCIR2, and the flow cytometry results indicate that αDEC205-OVA only bound to the CHO cell line expressing the mouse DEC205, while αDCIR2-OVA bound to the CHO cell line expressing the mouse DCIR2. As expected, the ISO-OVA did not bind to any cell line (Fig. S1B). In order to confirm the binding capacity of αDEC205-OVA and αDCIR2-OVA to murine splenic cDC1s and cDC2s, respectively, we performed a binding assay using splenocytes from WT mice. As expected, αDEC205-OVA preferentially bound to cDC1s, while αDCIR2-OVA bound specifically to cDC2s. The isotype control did not bind to any tested cDCs (Fig. S2). These results indicate that the chimeric αDEC205 and αDCIR2 are able to specifically target cDC1s and cDC2s, respectively.

3.3. STAT6 modulates cDC2-mediated T_{FH} cell responses

To analyze whether STAT6 signaling pathway would modulate the T_{FH} response promoted by antigen targeting to cDCs, we isolated DO11.10 $CD4^+$ T cells and adoptively transferred them to WT or STAT6 KO mice. After 24 h, we immunized mice with αDEC205-OVA, αDCIR2-OVA and ISO-OVA using Poly(I:C) as adjuvant, or only with Poly (I:C) as a negative control. As previously described, there is a pronounced increase in T_{FH} cell frequencies 5 days after immunization with the αDCIR2-OVA chimeric mAb (Sulczewski et al., 2020). We performed a flow cytometry analysis in the spleens to detect T_{FH} cells at this time point using the gating strategy described in Fig. S3. $CD19^-CD3^+CD4^+DO11.10^+CXCR5^+PD\text{-}1^+$ cells were gated to allow us to quantify the absolute number of T_{FH} cells per spleen. Our results indicate that T_{FH} cell numbers were increased in WT mice that received αDCIR2-OVA when compared to the other groups, confirming that antigen targeting to cDC2s via DCIR2 receptor induces T_{FH} cell priming (Fig. 2A). Of note, WT mice immunization with ISO-OVA also increased the numbers of T_{FH} cells when compared with WT mice that received αDEC205-OVA or only Poly (I:C). Interestingly, T_{FH} cell response was reduced in αDCIR2-OVA-immunized STAT6 KO mice, as the number of

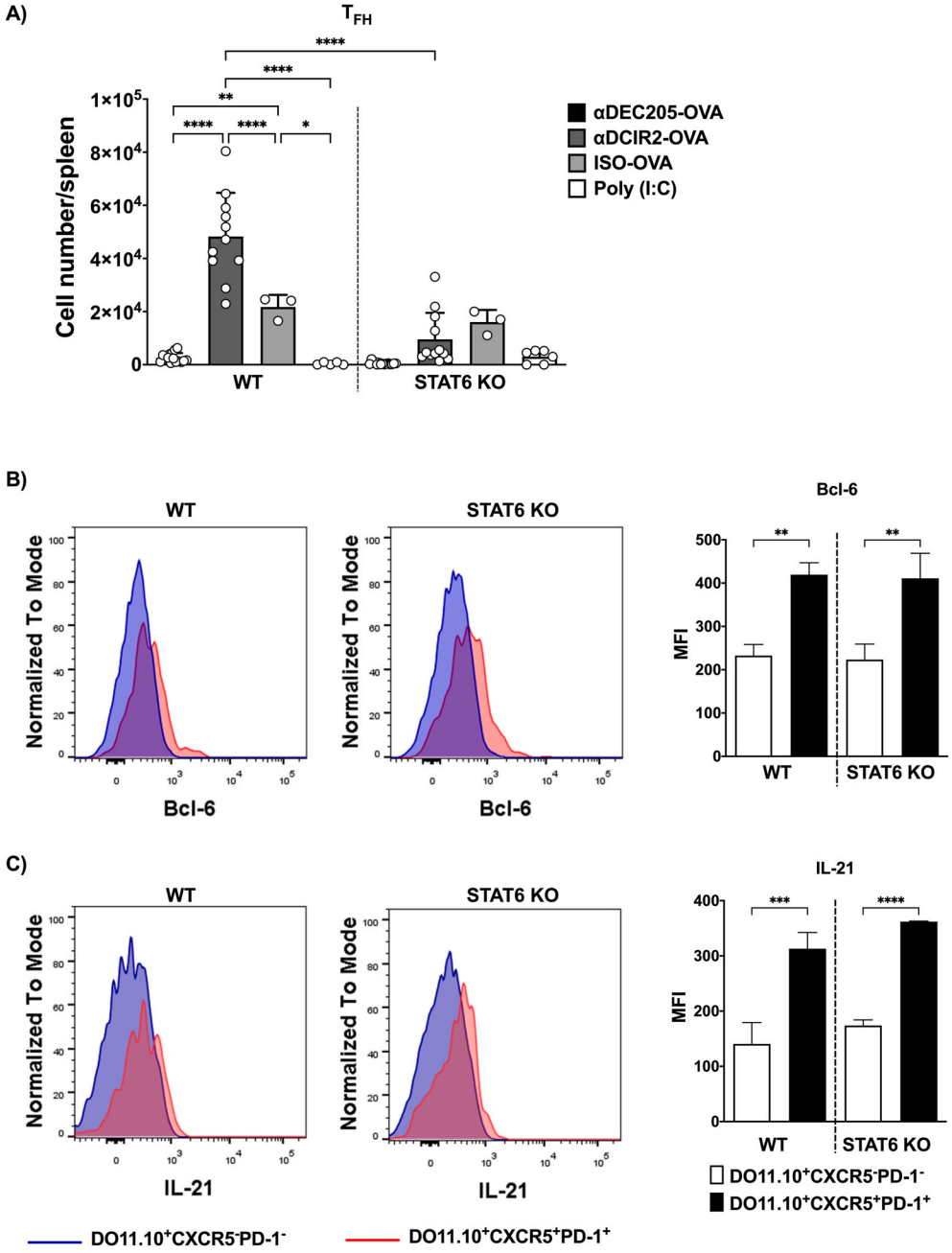

Fig. 2. T_{FH} cell priming after antigen targeting to cDCs. OVA-specific DO11.10 $CD4^+$ T cells were transferred to BALB/c WT or STAT6 KO mice that were immunized with 5 μg of αDEC-OVA, αDCIR2-OVA or ISO-OVA together with 50 μg of Poly (I:C) as adjuvant. Splenocytes were obtained 5 days after prime. T_{FH} cells were analyzed by flow cytometry. A) Absolute numbers of T_{FH} cells per spleen. Bcl-6 and IL-21 were stained after fixation and permeabilization and their expressions on T_{FH} cells were detected by flow cytometry. B) MFI for Bcl-6 was determined in T_{FH} ($CD3^+CD4^+DO11.10^+CXCR5^+PD\text{-}1^+$) and non-$T_{FH}$ cells ($CD3^+CD4^+$ $DO11.10^+CXCR5^-PD\text{-}1^-$). C) MFI for IL-21 was determined in T_{FH} ($CD3^+CD4^+$ $DO11.10^+CXCR5^+PD\text{-}1^+$) and non-$T_{FH}$ ($CD3^+CD4^+$ $DO11.10^+CXCR5^-PD\text{-}1^-$) cells. B–C). Histograms in blue show non-T_{FH} and in red T_{FH} cells. Bars show mean ± SD from five experiments pooled together (n = 3–12 animals/group) (A) or one experiment (n = 3 animals/group) (B–C). *p < 0.05, **p < 0.01, ***p < 0.001 and ****p < 0.0001; one-way ANOVA followed by Tukey's post-test. (For interpretation of the references to colour in this figure legend, the reader is referred to the Web version of this article.)

T_{FH} cells was significantly lower in STAT6 KO mice when compared to WT mice that received αDCIR2-OVA (Fig. 2A).

In an attempt to confirm that $CD19^{-}CD3^{+}CD4^{+}DO11.10^{+}CXCR5^{+}PD\text{-}1^{+}$ cells are indeed T_{FH} cells, we stained Bcl-6 and IL-21, the transcriptional factor responsible for the promotion of T_{FH} cell fate and the main cytokine secreted by these cells, respectively. In both mouse strains (WT and STAT6 KO), the MFI for Bcl-6 was significantly higher in $CD3^{+}CD4^{+}DO11.10^{+}CXCR5^{+}PD\text{-}1^{+}$ cells when compared to the MFI of $CD3^{+}CD4^{+}DO11.10^{+}$ cells that do not express CXCR5 and PD-1 (Fig. 2B and Fig. S3). Furthermore, our results also show that the MFI of IL-21, the main cytokine produced by T_{FH} cells, was also significantly higher in $CD3^{+}CD4^{+}DO11.10^{+}CXCR5^{+}PD\text{-}1^{+}$ cells (Fig. 2C). Thus, these results confirm that $CD3^{+}CD4^{+}DO11.10^{+}CXCR5^{+}PD\text{-}1^{+}$ cells are indeed T_{FH} cells.

To rule out the possibility that the reduced numbers of T_{FH} cells detected in STAT6 KO mice were due to lower expression of DCIR2 in cDC2s, we stained DEC205 and DCIR2 receptors in WT and STAT6 KO splenocytes to analyze their expression on cDC1s and cDC2s. We did not observe any statistical differences between the expression of either DEC205 or DCIR2 when we compared cDC1s and cDC2s from WT or STAT6 KO mice (Fig. S4). These results indicate that cDC2s from WT and STAT6 KO mice express similar levels of DCIR2 and the reduced T_{FH} cell response is not due to a defect in antigen targeting to cDC2s.

Taken together, our results show that the T_{FH} cell response promoted after antigen targeting to cDC2s via DCIR2 receptor is reduced in STAT6 KO mice, suggesting that the STAT6 signaling pathway stimulates T_{FH} cell fate in cDC2-mediated immune responses.

3.4. STAT6 signaling influences GC formation but not plasma cell differentiation

In an effort to better understand the role of STAT6 in the cDC2-

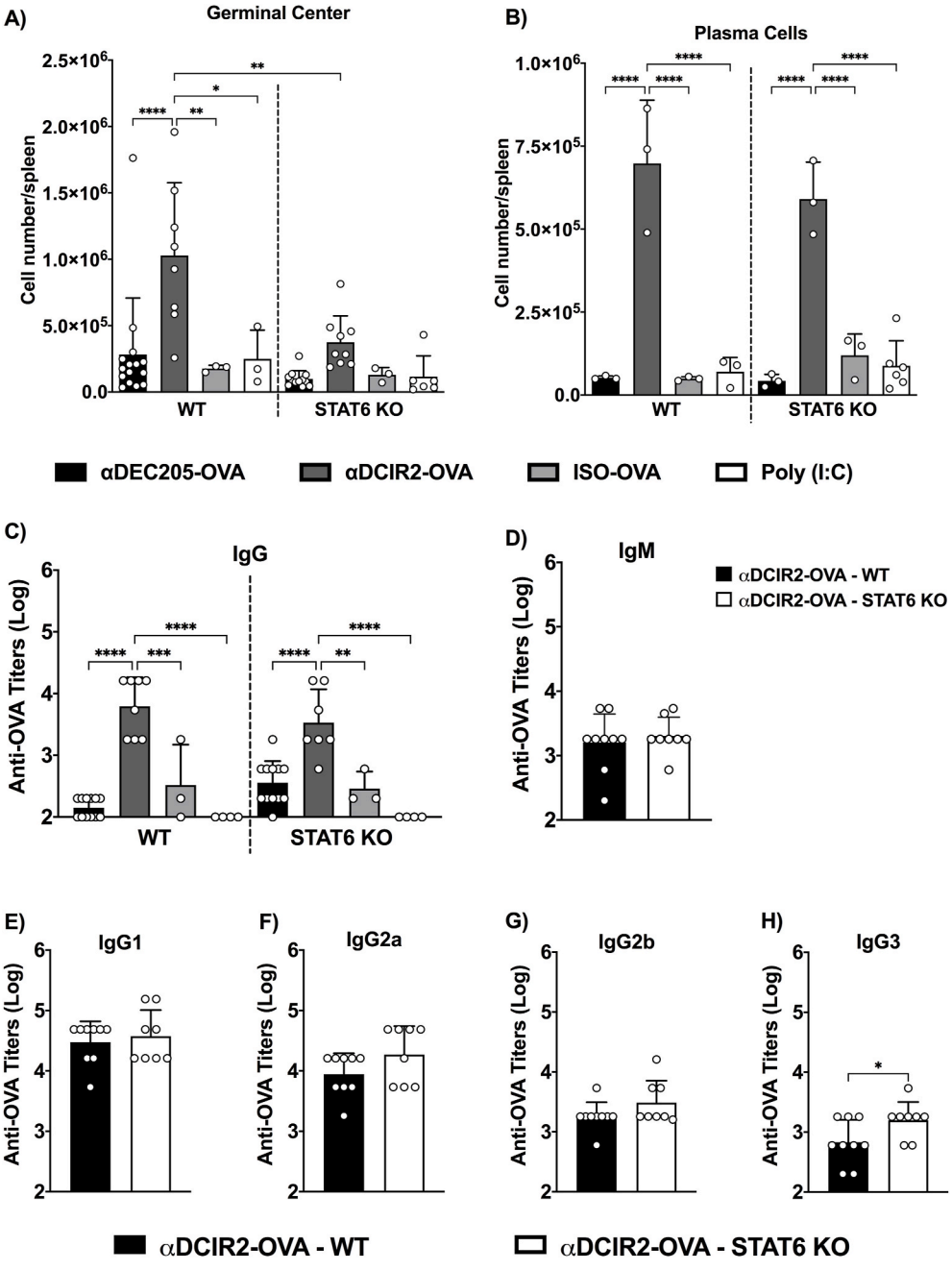

Fig. 3. Germinal center, plasma cells and antibody titers after antigen targeting to cDCs. WT and STAT6 KO mice were immunized as described in Fig. 2. Splenocytes were stained to detect GC B cells and plasma cells by flow cytometry. Absolute numbers of GC B cells (A) and plasma cells (B) per spleen. C–H) Sera were titrated to detect specific anti-OVA antibodies by ELISA. Anti-OVA IgG (C), IgM (D), IgG1 (E), IgG2a (F), IgG2b (G), and IgG3 (H) antibody titers five days after the immunization. Bars show mean ± SD from five experiments pooled together (n = 3–12 animals/group) in (A), from one representative experiment out of four independent experiments in (B) or from three experiments pooled together (n = 8–9 animals/group) in (C–H). *p < 0.05, **p < 0.01, ***p < 0.001 and ****p < 0.0001; one-way ANOVA followed by Tukey's post-test in (A–C) and Student's t-test in (D–H).

mediated immune response, we quantified the absolute number of GC B cells ($B220^{+}GL\text{-}7^{+}CD95^{+}$) and plasma cells ($B220^{Low}CD138^{High}$) according to the strategy detailed in Fig. S5. The absolute number of B cells in the GC was significantly increased only in WT αDCIR2-OVA-immunized mice when compared to the group that received only Poly (I:C). The STAT6 KO αDCIR2-OVA-immunized mice showed a statistically significant decrease in the number of GC B cells compared to the WT animals, indicating that STAT6 signaling pathway stimulates GC formation when the antigen is targeted to cDC2s via the DCIR2 receptor (Fig. 3A). Furthermore, this result suggests that the STAT6 signaling pathway modulates GC expansion.

Interestingly, when we analyzed the numbers of plasma cells in the spleen of WT and STAT6 KO mice immunized with αDEC205-OVA, αDCIR2-OVA, ISO-OVA or only Poly (I:C), plasma cell numbers in WT and STAT6 KO mice immunized with αDCIR2-OVA were statistically increased when compared to the other groups (Fig. 3B). These results confirm that antigen targeting to cDC2s promotes plasma cell differentiation 5 days after the immunization with αDCIR2-OVA and indicate that STAT6 does not influence plasma cell differentiation (Fig. 3B). In summary, in this model, GC and plasma cell differentiation occur in a STAT6-dependent and independent manner, respectively.

3.5. Anti-OVA antibody titers are not affected by the STAT6 signaling pathway

As plasma cells are antibody-producing cells, we tested whether STAT6 would interfere with antibody production. We analyzed the production of OVA-specific antibodies 5 days after antigen targeting to cDC1 and cDC2s via the DEC205 and DCIR2 receptors, respectively, in WT and STAT6 KO mice. As expected, the titers of anti-OVA IgG antibodies were significantly higher in αDCIR2-OVA-immunized WT and STAT6 KO mice. However, there were no significant differences in antibody titers between WT and STAT6 KO mice that received αDCIR2-OVA, showing that, in addition to not influencing the differentiation of antibody-producing cells (plasma cells), STAT6 signaling pathway also does not alter the production of IgGs (Fig. 3C).

As there was a decrease in GC B cells in STAT6 KO mice immunized with αDCIR2-OVA, we wondered whether STAT6 could change the class switch from IgM to IgG and also the switch of IgG subclasses. To investigate this, we performed an ELISA to quantify serum IgM, IgG1, IgG2a, IgG2b, and IgG3 titers in mice immunized with αDCIR2-OVA. The results showed that there were no statistical differences between the WT and STAT6 KO groups in terms of anti-OVA IgM, IgG1, IgG2a and

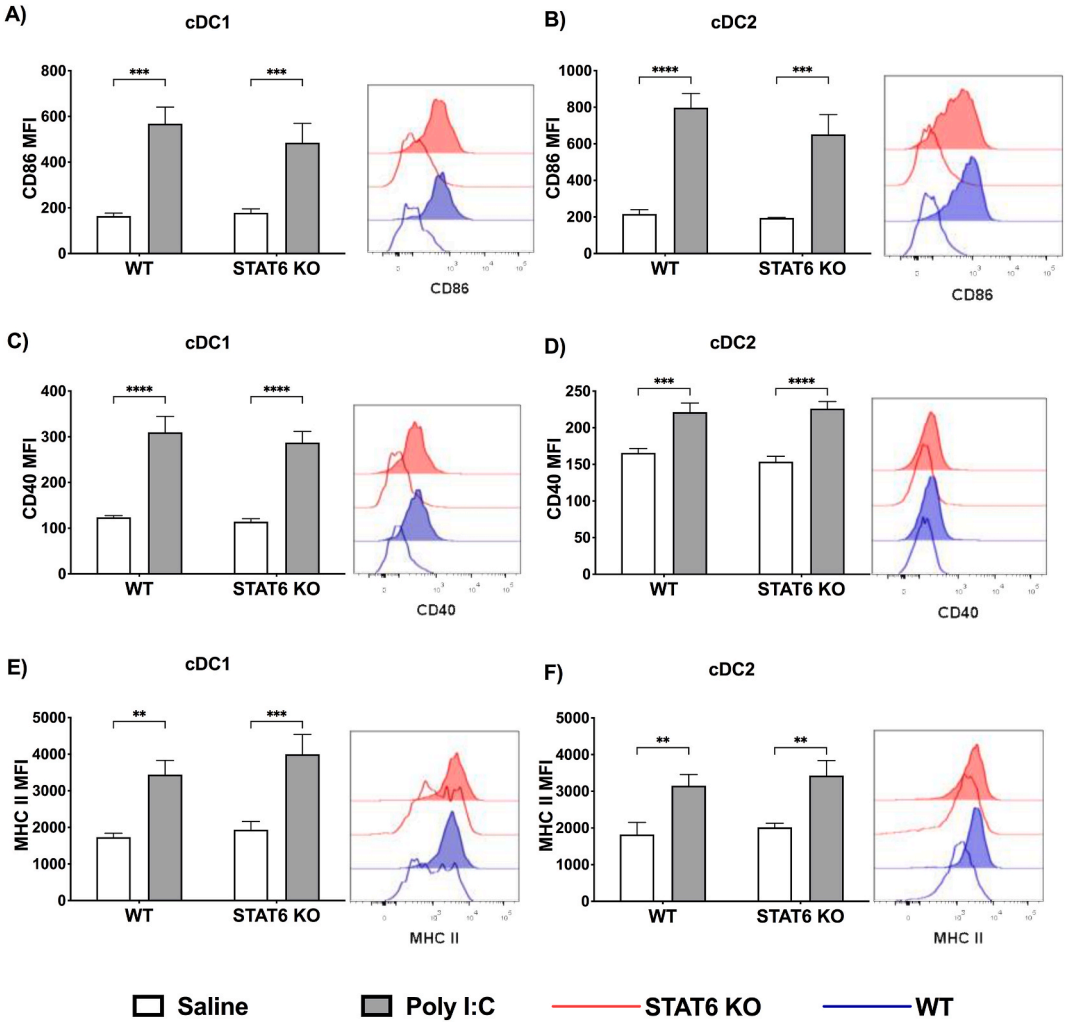

Fig. 4. Expression of co-stimulatory molecules CD86, CD40 and MHC II in cDC1s and cDC2s. Six hours after saline or Poly (I:C) administration, spleens from WT or STAT6 KO mice were removed, splenocytes were obtained and stained with different fluorochrome-conjugated antibodies. After sample acquisition, $CD19^{-}CD3^{-}MHCII^{+}CD11c^{+}$ cells were gated followed by $CD8\alpha^{+}CD11b^{-}$ (cDC1s) and $CD8\alpha^{-}CD11b^{+}$ (cDC2s). The median of fluorescence intensity (MFI) for CD86, CD40 and MHCII was analyzed in cDC1s (A-C-E) and cDC2s (B-D-F). Bars show mean ± SD of one representative experiment out of two independent experiments (n = 3 animals/group). Filled histograms represent WT (blue) or STAT6 KO (red) mice administered with Poly (I:C), while empty histograms represent WT (blue) or STAT6 KO (red) mice administered with saline. $^{**}p < 0.01$, $^{***}p < 0.001$ and $^{****}p < 0.0001$; one-way ANOVA followed by Tukey's post-test. (For interpretation of the references to colour in this figure legend, the reader is referred to the Web version of this article.)

IgG2b antibodies (Fig. 3D–G). We only detected a slight increase in IgG3 titers in the STAT6 KO group compared to WT (Fig. 3H).

To complement these results, we also analyzed the antibody titers, in WT and STAT6 KO mice, 14 days after the administration of one dose (priming) of αDCIR2-OVA plus poly (I:C), or 7 and 14 days after the administration of a second dose (boost) with αDCIR2-OVA alone. Total IgG, IgG1, IgG2a, IgG2b, and IgG3 titers were tested 14 days after priming, and 7 and 14 days after boost. Our results again indicated that the antibody titers for total IgG, IgG1, IgG2a and IgG2b were similar in WT and STAT6 KO mice at all time points tested. IgG3 titers were still higher in STAT6-deficient mice 14 days after priming and 7 days after boosting (Fig. S6).

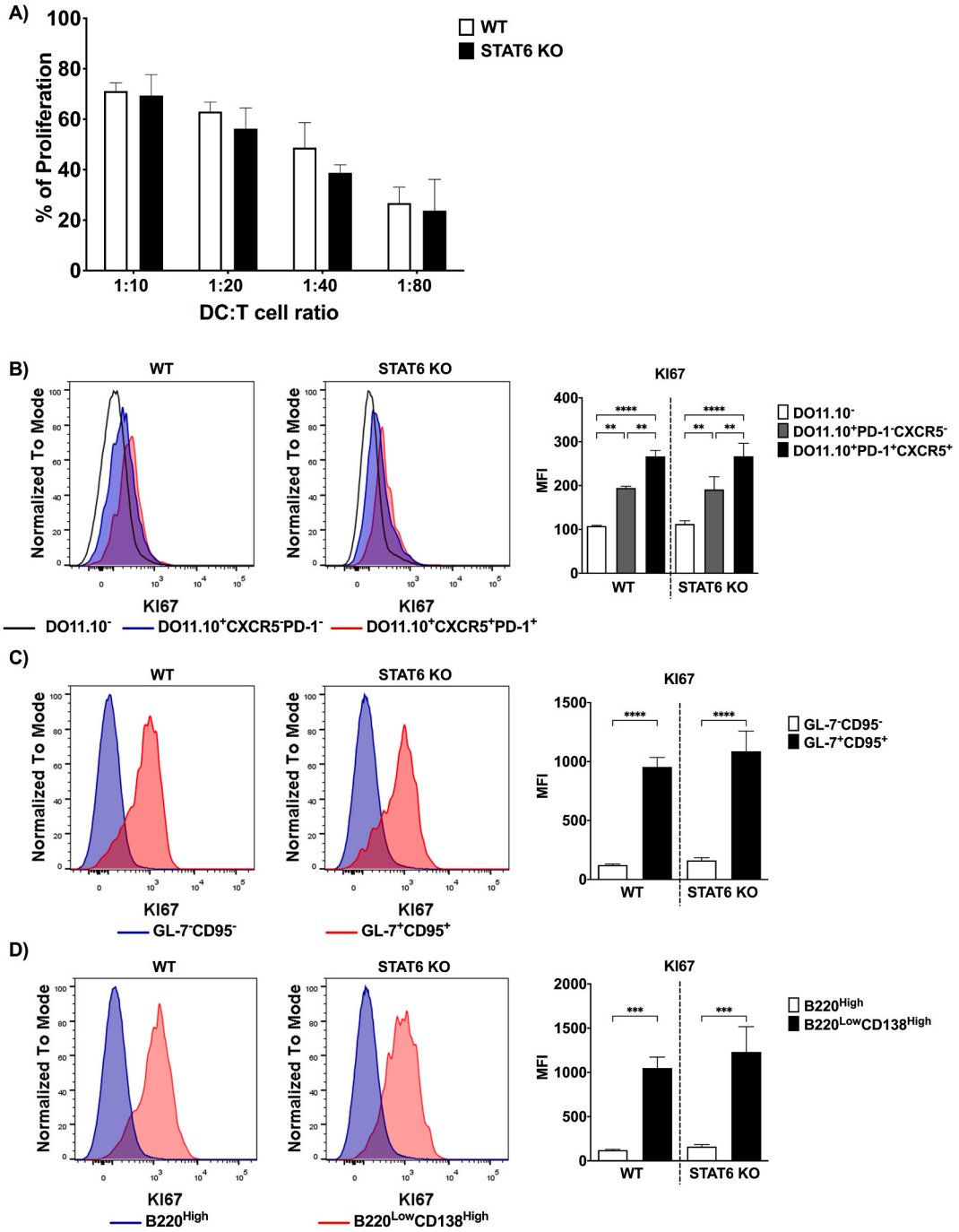

Fig. 5. Proliferation of $CD4^+$ T cells co-cultured with WT and STAT6 KO cDC2s. A) cDC2s from WT and STAT6 KO mice were isolated, pulsed *in vitro* with 10 μg/mL of OVA and stimulated with Poly (I:C). Then, they were co-cultured with CFSE-labeled $CD4^+$ DO11.10 T cells. cDC2s were added in different DC:T proportions (1:10, 1:20, 1:40 and 1:80). After five days in culture, the proliferation of $CD4^+$ T cells was analyzed by CFSE dilution. A) Frequency of $CFSE^{low}$ cells in $CD4^+$ $DO11.10^+$ T cells cultured in different DC:T cells proportions. Intranuclear KI67 staining was performed in splenocytes from WT and STAT6 KO mice immunized with αDCIR2-OVA as described in Fig. 2. B) KI67 MFIs were detected in T_{FH} cells (red histograms), non-T_{FH} cells (blue histograms) or non-DO11.10 cells (white histograms). C) KI67 MFIs were detected in GC (red histograms) or in regular B cells (blue histograms). D) KI67 MFIs were detected in plasma cells (red histograms) or non-plasma cells (blue histograms) by flow cytometry. Bars show mean ± SD results from one representative experiment out of two independent experiments (n = 3 animals/group). $^{**}p < 0.01$, $^{***}p < 0.001$ and $^{****}p < 0.0001$; one-way ANOVA followed by Tukey's post-test. (For interpretation of the references to colour in this figure legend, the reader is referred to the Web version of this article.)

3.6. STAT6 signaling does not influence the maturation of cDCs

The reduced response of T_{FH} cells in the absence of STAT6 led us to evaluate whether the STAT6 signaling pathway would influence Poly (I:C)-promoted cDC maturation. We then administered Poly (I:C) or only saline to WT and STAT6 KO mice. After 6 h, the splenocytes were stained for the analysis of CD86, CD40 and MHCII in cDC1s and cDC2s. In cDC1s, *in vivo* administration of Poly (I:C) increased the MFI for the costimulatory molecules CD86 and CD40 and for MHCII when compared with the group that received only saline (Fig. 4). When we compared the WT and STAT6 KO mice that received Poly (I:C), no differences were observed when we evaluated the MFIs for CD86, CD40, and MHCII in cDC1s (Fig. 4A-C-E). These results indicate that the STAT6 signaling pathway does not influence the maturation profile of cDC1s in the spleen. In the same way, we detected an increase in the MFI of CD86, CD40 and MHCII in cDC2s from mice that received Poly (I:C), when compared to the ones that received saline. No differences were observed when WT and STAT6 KO mice that received Poly (I:C) were compared (Fig. 4B-D-F). Therefore, the STAT6 signaling pathway does not modulate the maturation of cDC2s *in vivo* after Poly (I:C) injection.

3.7. STAT6 signaling does not alter proliferation of $CD4^+$ T cells

In attempt to unravel the mechanism that induces the reduced T_{FH} cell response in αDCIR2-OVA-immunized STAT6 KO mice, we investigated whether STAT6-deficient cDC2s would fail to promote $CD4^+$ T cell proliferation. To perform the experiment, we isolated OVA-specific DO11.10 $CD4^+$ T cells and WT and STAT6 KO cDC2s using cell sorting. cDC2s were pulsed *in vitro* with OVA and then cocultured with DO11.10 $CD4^+$ T cells in different proportions of DC-T cells (1:10, 1:20: 1:40 and 1:80). Five days later, we analyzed DO11.10 $CD4^+$ T cell proliferation by CFSE dilution. The results showed that there were no significant differences in the proliferation of DO11.10 $CD4^+$ T cells that were cocultured with cDC2s STAT6-deficient or not (Fig. 5A). Thus, the STAT6 signaling pathway does not influence the ability of cDC2s to promote $CD4^+$ T cell proliferation *in vitro*.

To confirm this result, we also analyzed the proliferation of DO11.10 $CD4^+$ T cells *in vivo* after antigen targeting to WT or STAT6 KO cDC2s via the DCIR2 receptor. To do that, we evaluated the intranuclear expression of KI67 in DO11.10 T_{FH} cells ($DO11.10^+PD\text{-}1^+CXCR5^+$) from WT and STAT6 KO mice immunized with αDCIR2-OVA plus Poly (I:C). As controls, we compared KI67 MFIs of $DO11.10^+PD\text{-}1^-CXCR5^-$ and $DO11.10^-$ cells that did not proliferate in response to OVA (Fig. 5B). KI67 MFIs were significantly higher in DO11.10 cells ($DO11.10^+PD1^+CXCR5^+$ and $DO11.10^+PD\text{-}1^-CXCR5^-$ cells) transferred when compared to MFIs of self-$CD4^+$ T cells ($DO11.10^-$ cells) from both WT and STAT6 KO mice. The results also showed that KI67 MFIs in T_{FH} cells were significantly higher than in non-T_{FH} $DO11.10^+$ cells, indicating that $DO11.10^+CXCR5^+PD\text{-}1^+$ (T_{FH}) cells proliferate more than cells that do not express CXCR5 and PD1. Furthermore, T_{FH} cells from WT mice or STAT6 KO mice showed similar KI67 MFIs, suggesting that, although STAT6 KO animals show a decrease in the number of T_{FH} cells, these cells do not show any defect in their proliferation capacity (Fig. 5B). These results suggest that the decrease in the number of T_{FH} cells does not occur due to a difference in proliferation capacity of these cells, suggesting that, in both cases, the OVA-specific $DO11.10^+$ $CD4^+$ T cells were similarly activated by WT and STAT6 KO cDC2s.

3.8. GC and plasma cell proliferation are not affected by the STAT6 signaling pathway

We also analyzed the proliferation of GC B cells and plasma cells to figure out if B cell proliferation is impaired in STAT6 KO mice. The results show that GC B cells and plasma cells have a significantly higher KI67 MFI than B cells that do not express GL-7 and CD95 or CD138, suggesting that GC B cells and plasma cells proliferate more than other B cells, as expected. When comparing KI67 MFIs of GC B cells and plasma cells from WT or STAT6 KO mice, our results indicated that there were no significant differences between these two groups, suggesting that GC B cells and plasma cells from STAT6 KO mice proliferate similarly to GC B cells and plasma cells from WT mice (Fig. 5C and D).

3.9. Atypical frequency of GC B cells in the light zone of STAT6-deficient mice

Reduced numbers and normal proliferation of T_{FH} and GC B cells in STAT6 KO mice led us to hypothesize that the STAT6 signaling pathway may control the dynamics of GC. To address this question, we analyzed the frequencies of light zone or dark zone B cells in WT and STAT6 KO mice after immunization with αDCIR2-OVA. Five days after immunization, the spleen cells were harvested and light and dark zone GC cells were stained with CD83 ($B220^+GL\text{-}7^+CD95^+CD83^+$) and CXCR4 ($B220^+GL\text{-}7^+CD95^+CXCR4^+$), respectively (Fig. 6A). The results showed that the frequencies of dark zone GC cells were similar between WT and STAT6 KO mice. Interestingly, the frequency of GC B cells in the light zone was increased in STAT6-deficient mice (Fig. 6B). These results indicate that light zone GC B cells accumulated in STAT6-deficient mice, suggesting that the STAT6 signaling pathway influences GC dynamics.

4. Discussion

In recent years, much evidence has been gathered indicating that cDC2s are specialized to prime T_{FH} cells (Briseno et al., 2018; Chappell et al., 2012; Krishnaswamy et al., 2017; Li et al., 2016; Shin et al., 2015, 2016; Sulczewski et al., 2020). Interestingly, both resident and migratory cDC2s appear to preferentially prime T_{FH} cells (Krishnaswamy et al., 2017; Shin et al., 2015; Sulczewski et al., 2020). Non-coincidentally, cDC2s localize in the outer part of the T cell zone and to the marginal zone, a place close to the B cell zone in lymph nodes and spleen (Calabro et al., 2016b; Krishnaswamy et al., 2017). This is a place that supports all the interactions required for T_{FH} cell fate and GC formation, resulting in antibody production and affinity maturation (Eisenbarth, 2019; Mesin et al., 2016). Part of the evidence showing that cDC2s are specialized in T_{FH} cell priming was obtained in studies using antigen targeting to cDCs, a strategy that promotes humoral and cellular immune responses. Antigen targeting to cDC2s via the DCIR2 receptor promotes T_{FH} cell fate, GC formation, and plasma cell differentiation (Chappell et al., 2012; Shin et al., 2015; Sulczewski et al., 2020).

Although much effort was made to identify cDC-promoted immune responses after antigen targeting via DEC205 and DCIR2 receptors, we still do not fully understand the mechanisms that coordinate adaptive immunity induction after immunization with αDEC205 and αDCIR2 chimeric mAbs. Here, we took advantage of this antigen targeting strategy to study whether STAT6 signaling pathway could modulate the immune response promoted by cDCs. We immunized WT and STAT6 KO mice with the αDEC205 and αDCIR2 mAbs linked with Ovalbumin using Poly (I:C) as an adjuvant.

First, we analyzed whether STAT6 depletion would change the development of cDCs *in vivo*. Although IL-4, which promotes STAT6 phosphorylation, is widely used in combination with GM-CSF to generate DC-like cells (bone marrow-derived dendritic cells) *in vitro,* our findings indicate that STAT6-deficient mice do not have an impaired splenic development of cDC1s and cDC2s *in vivo*, indicating that differentiation of cDCs occurs in a STAT6 independent-manner (Matheu et al., 2008; Menges et al., 2005; Vento-Tormo et al., 2016). In fact, the main cytokines that regulate cDC development *in vivo,* FLT3L and GM-CSF, signal though STAT3 and STAT5, respectively (Esashi et al., 2008; Laouar et al., 2003). Our data still add evidence that *in vitro*--generated DC-like cells do not follow the same differentiation pathway followed by cDC1s and cDC2s found *in vivo* (Cabeza-Cabrerizo et al., 2021; Vento-Tormo et al., 2016).

Following the same reasoning, cDC maturation in response to Poly (I:

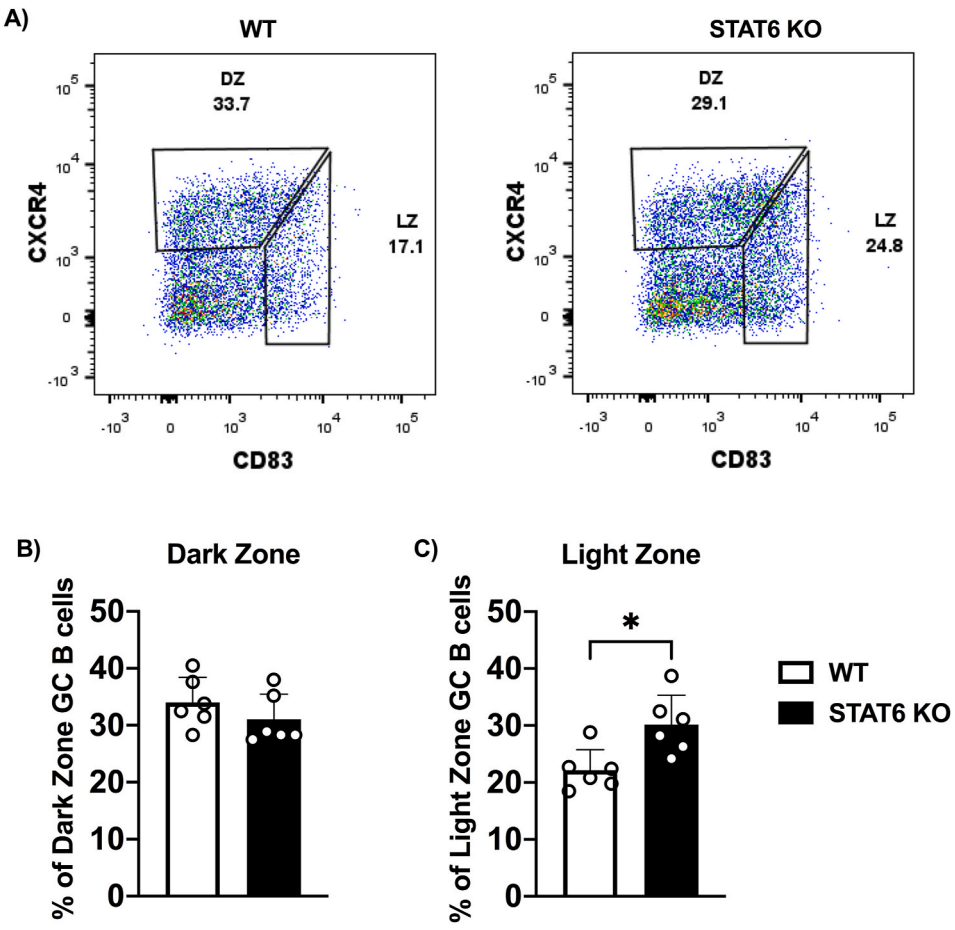

Fig. 6. Light and Dark zone B cell frequencies in GCs after antigen targeting to cDC2s via DCIR2 Receptor. Mice were immunized with αDCIR2-OVA together with 50 μg of Poly (I:C) as adjuvant. Splenocytes were obtained 5 days after prime and stained to detect GC B cells from light ($CD83^+$ cells) and dark ($CXCR4^+$ cells) zones by flow cytometry. A) representative dot plots from WT and STAT6 KO mice indicating light and dark zone B cell frequencies in GC B cells ($CD3^-B220^+GL\text{-}7^+CD95^+$). Frequencies of splenic dark zone GC B cells (B) and light zone GC B cells (C) in WT and STAT6 KO mice. Bars show mean ± SD from two representative experiments pooled together (n = 6 animals/group). *p < 0.05; Student's t-test.

C) was not affected by STAT6 deficiency in cDC1s and cDC2s, as both subsets upregulated CD86, CD40, and MHCII when WT and STAT6 KO mice received Poly (I:C). Nonetheless, it is important to point out that Poly (I:C) administration *in vivo* promotes cDC1s and cDC2s maturation mainly though cytokine signaling. Although cDC1s express higher amounts of TLR3, which recognizes Poly (I:C), these cells are essentially matured through type I interferons after *in vivo* injection of Poly (I:C) (Edwards et al., 2003; Trumpfheller et al., 2008). On the contrary, cDC2s, which do not express TLR3, are stimulated via another pathway, TNF-α and IL-6 synergically stimulate the up-regulation of costimulatory molecules and consequently the migration of cDC2s in response to Poly (I:C) (Edwards et al., 2003; Garcias Lopez et al., 2020).

Mature cDC2s migrate to the most external part of the T cell zone, near the B cell zone (Calabro et al., 2016b). This microenvironment is strategic for the induction of T_{FH} cell responses, especially after antigen targeting to cDC2s via DCIR2 receptor (Chappell et al., 2012). Here we confirm previous findings that cDC2s are specialized to prime T_{FH} cells (Shin et al., 2015; Sulczewski et al., 2020), as αDCIR2-OVA-immunized mice promoted a robust T_{FH} cell response that supported GC formation. Interestingly, STAT6-deficient mice were unable to promote T_{FH} and GC responses, indicating that the STAT6 signaling pathway positively modulates the fate of T_{FH} and CG cells when the antigen is targeted to cDC2s. In addition, our data also show that cDC2s' ability to promote $CD4^+$ T cell proliferation, including the proliferation of T_{FH} cells, is not dependent on STAT6 signaling. However, cDC2s are capable of priming T_{FH} in the absence of adjuvant, suggesting that the specialization of cDC2s to promote T_{FH} responses may not depend on inflammation or any cytokine (Chappell et al., 2012; Shin et al., 2015). In fact, cDC2s prime T_{FH} cells when they are stimulated with different adjuvants, such as LPS, Poly (I:C), and CpG, demonstrating that their role in T_{FH} cell priming may depend on cDC2-intrinsic biology (Chappell et al., 2012; Shin et al., 2015, 2016; Sulczewski et al., 2020). Of note, we did not address the role of other adjuvants in our system and cannot rule out the possibility that the reduced T_{FH} and GC responses in STAT6-deficient mice were due to Poly (I:C)-specific signaling. However, this does not appear to be the case because reduced GC responses were also detected in STAT6-deficient mice infected with *Nippostrongylus brasiliensis* or immunized with NP-ovalbumin in *alum* (Gonzalez et al., 2018; Turqueti-Neves et al., 2014).

It should also be mentioned that our results showed that immunization of WT mice with ISO-OVA and Poly (I:C) induced a significant increase in T_{FH} but not in GC B cells. This inconsistency may be due to the system we chose: OVA-specific DO11.10 $CD4^+$ T cell transference before immunization. Experiments with another OVA-specific transgenic T cell (OT-II) did not show priming of T_{FH} cells or GC expansion after immunization with ISO-OVA (Kato et al., 2015). Indeed, our group has also reported no increase in T_{FH} cells or in GC B cells when ISO--$MSP1_{19}$PADRE was used to immunize WT mice that were not transferred with any transgenic T cell (Sulczewski et al., 2020).

Apparently, $CD4^+$ T cell proliferation after antigen targeting to cDC2s through the DCIR2 receptor is sustained by B cells, even though GC, plasma cell differentiation, and antibody production occur in a T cell-dependent manner (Chappell et al., 2012; Sulczewski et al., 2020). Considering that B-T cell interactions are also required for T_{FH} cell priming, our results indicate that there was a decrease in the GC response in STAT6 KO mice, suggesting that perhaps STAT6 deficiency influences interactions between B and T cells. There is evidence suggesting that GC in STAT6 KO or IL-4/IL-13 KO mice are smaller compared to GC in WT mice, indicating that the STAT6 signaling pathway modulates the ability of B cells to promote expansion of GC

(Gonzalez et al., 2018; Turqueti-Neves et al., 2014). We also tested whether STAT6 would alter GC B cells proliferation, and our results indicated that the reduced GC B cell numbers were not due to an impaired proliferation of GC B cells. This result is in agreement with a previous study that also showed that IL-4 deficiency does not alter proliferation or promotes apoptosis in GC B cells (Gonzalez et al., 2018).

Furthermore, STAT6 appears to influence B cell migration between the light zone and dark zones (Gonzalez et al., 2018). In this way, it could lead to a reduction in the size of the GC and consequently to a decrease in the number of GL-7^{+}CD95^{+} B cells and also T_{FH} cells, as we report here. In an attempt to address whether STAT6 would have an effect on GC dynamics, we decided to check the frequencies of GC B cells from the light and the dark zones in WT and STAT6-deficient mice. Our data showed that STAT6 KO mice accumulated GC B cells in the light zone, thus suggesting that these mice may have an abnormal proportion of GC B cells in the light and dark zones. In this way, STAT6 may influence the dynamics that promotes GC expansion. It is worth noting that B cells localized in the light zone do not proliferate, as the light zone is responsible for reducing the number of B cells in the GC through mechanisms of clonal selection (Mesin et al., 2016).

Another study showed that STAT6 may help in the correct positioning of B cells in the GC due to the decreased expression of EBI2 in B cells, which impairs the migration of these cells into the GC (Gatto et al., 2009; Pereira et al., 2009; Turqueti-Neves et al., 2014). Thus, our results confirm that the STAT6 signaling pathway stimulates the expansion of the GC, in addition to providing evidence that STAT6 does not influence the function of cDC2s to prime T_{FH} cells, but regulates the traffic or the positioning of B cells into the GC.

Finally, our analyses indicate that STAT6 KO and WT mice have similar numbers of plasma cells after antigen targeting to cDC2 through the DCIR2 receptor. We also show that STAT6-deficient plasma cells proliferate equally as WT cells. Interestingly, even with a smaller GC, our findings suggest that plasma cell differentiation occurs independently of STAT6. They indicate that early plasma cell response induced by antigen targeting to cDC2s via DCIR2 receptor may not emerge from GCs that are known to generate high affinity plasma cells (Viant et al., 2020). In fact, the early B cell response promoted by immunization with αDCIR2 is driven by extrafollicular B cells that induce T cell proliferation (Chappell et al., 2012). Our findings allow us to speculate that plasma cells induced by αDCIR2-OVA immunization may be extrafollicular and probably short-lived antibody producing cells as well. We did not find plasma cells in the spleen in longer time points after antigen targeting to cDC2s via DCIR2 (Sulczewski et al., 2020). Therefore, it is not surprising that the number of plasma cells was not affected by the reduction of the GC response. It is also important to point out that previous findings indicate that plasma cell differentiation happens in a CD4^{+} T cell-dependent manner (Sulczewski et al., 2020). The results presented here show that decreased numbers of T_{FH} cells support plasma cell differentiation. Further research is necessary to better understand the differentiation of plasma cells after antigen targeting to cDC2s via DCIR2.

In addition, anti-OVA IgG production was also not affected in STAT6 KO mice (except IgG3) over time. The analysis of different IgG subtypes indicated that WT and STAT6 KO produced total IgG, IgG1, IgG2a and IgG2b in a similar way at different time points after one or two doses of αDCIR2-OVA. These results suggest that STAT6 does not influence IgG subtype switch, except IgG3 that accumulated in the serum of STAT6 KO mice up to at least 7 days after the boosting dose. Recent findings support the idea that the switch in antibody class occurs in extrafollicular regions of secondary lymphoid organs (Roco et al., 2019). This fact may explain why the titers of IgG1, IgG2a and IgG2b were not affected by STAT6 depletion, although GC were reduced in STAT6-deficient mice. It also supports the hypothesis that plasma cells are generated by extrafollicular B cells. Furthermore, reduced GC may affect antibody affinity, mainly at longer time points. New analyses are required to clear out the impact of smaller GCs on antibody affinity over time.

In summary, our results indicate that the STAT6 signaling pathway plays a role in the development of T_{FH} and germinal centers when the antigen is targeted to cDC2s through the DCIR2 receptor.

CRediT authorship contribution statement

Fernando Bandeira Sulczewski: Conceptualization, Data curation, Formal analysis, Investigation, Validation, Methodology, Writing – original draft, Visualization. **Larissa Alves Martino:** Methodology, Validation. **Bianca da Silva Almeida:** Methodology. **Márcio Massao Yamamoto:** Methodology. **Daniela Santoro Rosa:** Conceptualization, Methodology, Resources, Writing – review & editing. **Silvia Beatriz Boscardin:** Conceptualization, Methodology, Resources, Writing – review & editing, Visualization, Supervision, Project administration, Funding acquisition.

Declaration of competing interest

The authors declare that they have no known competing financial interests or personal relationships that could have appeared to influence the work reported in this paper.

Acknowledgments

This research was supported by the Sao Paulo Research Foundation (FAPESP, grant #2018/07142-9 and 2017/17471-7), the Brazilian National Research Council (CNPq, grant #440721/2016-4), and the Coordination for the Improvement of Higher Level Personnel (CAPES, grant #2047/2016). FBS, BSA and LAM received fellowships from FAPESP (2018/00145–2, 2017/26342–6 and 2018/20821–2, respectively). DSR and SBB received fellowships from CNPq.

The authors would like to thank Dr. Luís Carlos de Sousa Ferreira for access to the cytometer, and Danielle Chagas, Bruno de Castro Bertoldo and Anderson Domingos Silva for assistance in the animal facility.

Appendix A. Supplementary data

Supplementary data to this article can be found online at https://doi.org/10.1016/j.crimmu.2021.08.001.

References

Amorim, K.N.S., Chagas, D.C.G., Sulczewski, F.B., Boscardin, S.B., 2016. Dendritic cells and their multiple roles during malaria infection. Journal of Immunology Research 2926436, 2016.

Anderson 3rd, D.A., Dutertre, C.A., Ginhoux, F., Murphy, K.M., 2020. Genetic models of human and mouse dendritic cell development and function. Nat. Rev. Immunol.

Antonialli, R., Sulczewski, F.B., Amorim, K., Almeida, B.D.S., Ferreira, N.S., Yamamoto, M.M., Soares, I.S., Ferreira, L.C.S., Rosa, D.S., Boscardin, S.B., 2017. CpG oligodeoxinucleotides and flagellin modulate the immune response to antigens targeted to CD8alpha(+) and CD8alpha(-) conventional dendritic cell subsets. Front. Immunol. 8, 1727.

Ardouin, L., Luche, H., Chelbi, R., Carpentier, S., Shawket, A., Montanana Sanchis, F., Santa Maria, C., Grenot, P., Alexandre, Y., Gregoire, C., et al., 2016. Broad and largely concordant molecular changes characterize tolerogenic and immunogenic dendritic cell maturation in thymus and periphery. Immunity 45, 305–318.

Ballesteros-Tato, A., Leon, B., Graf, B.A., Moquin, A., Adams, P.S., Lund, F.E., Randall, T. D., 2012. Interleukin-2 inhibits germinal center formation by limiting T follicular helper cell differentiation. Immunity 36, 847–856.

Banchereau, J., Steinman, R.M., 1998. Dendritic cells and the control of immunity. Nature 392, 245–252.

Bonifaz, L., Bonnyay, D., Mahnke, K., Rivera, M., Nussenzweig, M.C., Steinman, R.M., 2002. Efficient targeting of protein antigen to the dendritic cell receptor DEC-205 in the steady state leads to antigen presentation on major histocompatibility complex class I products and peripheral CD8+ T cell tolerance. J. Exp. Med. 196, 1627–1638.

Bonifaz, L.C., Bonnyay, D.P., Charalambous, A., Darguste, D.I., Fujii, S., Soares, H., Brimnes, M.K., Moltedo, B., Moran, T.M., Steinman, R.M., 2004. In vivo targeting of antigens to maturing dendritic cells via the DEC-205 receptor improves T cell vaccination. J. Exp. Med. 199, 815–824.

Boscardin, S.B., Hafalla, J.C., Masilamani, R.F., Kamphorst, A.O., Zebroski, H.A., Rai, U., Morrot, A., Zavala, F., Steinman, R.M., Nussenzweig, R.S., Nussenzweig, M.C., 2006. Antigen targeting to dendritic cells elicits long-lived T cell help for antibody responses. J. Exp. Med. 203, 599–606.

Bottcher, J.P., Bonavita, E., Chakravarty, P., Blees, H., Cabeza-Cabrerizo, M., Sammicheli, S., Rogers, N.C., Sahai, E., Zelenay, S., Reis, E.S.C., 2018. NK cells stimulate recruitment of cDC1 into the tumor microenvironment promoting cancer immune control. Cell 172, 1022–1037 e1014.

Briseno, C.G., Satpathy, A.T., Davidson, J.T.t., Ferris, S.T., Durai, V., Bagadia, P., O'Connor, K.W., Theisen, D.J., Murphy, T.L., Murphy, K.M., 2018. Notch2-dependent DC2s mediate splenic germinal center responses. Proc. Natl. Acad. Sci. U. S. A. 115, 10726–10731.

Cabeza-Cabrerizo, M., Cardoso, A., Minutti, C.M., Pereira da Costa, M., Reis, E.S.C., 2021. Dendritic cells revisited. Annu. Rev. Immunol.

Calabro, S., Gallman, A., Gowthaman, U., Liu, D., Chen, P., Liu, J., Krishnaswamy, J.K., Nascimento, M.S., Xu, L., Patel, S.R., et al., 2016a. Bridging channel dendritic cells induce immunity to transfused red blood cells. J. Exp. Med. 213, 887–896.

Calabro, S., Liu, D., Gallman, A., Nascimento, M.S., Yu, Z., Zhang, T.T., Chen, P., Zhang, B., Xu, L., Gowthaman, U., et al., 2016b. Differential intrasplenic migration of dendritic cell subsets tailors adaptive immunity. Cell Rep. 16, 2472–2485.

Chappell, C.P., Draves, K.E., Giltiay, N.V., Clark, E.A., 2012. Extrafollicular B cell activation by marginal zone dendritic cells drives T cell-dependent antibody responses. J. Exp. Med. 209, 1825–1840.

Crotty, S., 2011. Follicular helper CD4 T cells (TFH). Annu. Rev. Immunol. 29, 621–663.

Do, Y., Koh, H., Park, C.G., Dudziak, D., Seo, P., Mehandru, S., Choi, J.H., Cheong, C., Park, S., Perlin, D.S., et al., 2010. Targeting of LcrV virulence protein from Yersinia pestis to dendritic cells protects mice against pneumonic plague. Eur. J. Immunol. 40, 2791–2796.

Dudziak, D., Kamphorst, A.O., Heidkamp, G.F., Buchholz, V.R., Trumpfheller, C., Yamazaki, S., Cheong, C., Liu, K., Lee, H.W., Park, C.G., et al., 2007. Differential antigen processing by dendritic cell subsets in vivo. Science 315, 107–111.

Edwards, A.D., Diebold, S.S., Slack, E.M., Tomizawa, H., Hemmi, H., Kaisho, T., Akira, S., Reis e Sousa, C., 2003. Toll-like receptor expression in murine DC subsets: lack of TLR7 expression by CD8 alpha+ DC correlates with unresponsiveness to imidazoquinolines. Eur. J. Immunol. 33, 827–833.

Eisenbarth, S.C., 2019. Dendritic cell subsets in T cell programming: location dictates function. Nat. Rev. Immunol. 19, 89–103.

Esashi, E., Wang, Y.H., Perng, O., Qin, X.F., Liu, Y.J., Watowich, S.S., 2008. The signal transducer STAT5 inhibits plasmacytoid dendritic cell development by suppressing transcription factor IRF8. Immunity 28, 509–520.

Garcias Lopez, A., Bekiaris, V., Muller Luda, K., Hutter, J., Ulmert, I., Getachew Muleta, K., Nakawesi, J., Kotarsky, K., Malissen, B., O'Keeffe, M., et al., 2020. Migration of murine intestinal dendritic cell subsets upon intrinsic and extrinsic TLR3 stimulation. Eur. J. Immunol. 50, 1525–1536.

Gatto, D., Paus, D., Basten, A., Mackay, C.R., Brink, R., 2009. Guidance of B cells by the orphan G protein-coupled receptor EBI2 shapes humoral immune responses. Immunity 31, 259–269.

Gatto, D., Wood, K., Caminschi, I., Murphy-Durland, D., Schofield, P., Christ, D., Karupiah, G., Brink, R., 2013. The chemotactic receptor EBI2 regulates the homeostasis, localization and immunological function of splenic dendritic cells. Nat. Immunol. 14, 446–453.

Gonzalez, D.G., Cote, C.M., Patel, J.R., Smith, C.B., Zhang, Y., Nickerson, K.M., Zhang, T., Kerfoot, S.M., Haberman, A.M., 2018. Nonredundant roles of IL-21 and IL-4 in the phased initiation of germinal center B cells and subsequent self-renewal transitions. J. Immunol. 201, 3569–3579.

Guilliams, M., Dutertre, C.A., Scott, C.L., McGovern, N., Sichien, D., Chakarov, S., Van Gassen, S., Chen, J., Poidinger, M., De Prijck, S., et al., 2016. Unsupervised high-dimensional analysis aligns dendritic cells across tissues and species. Immunity 45, 669–684.

Guilliams, M., Ginhoux, F., Jakubzick, C., Naik, S.H., Onai, N., Schraml, B.U., Segura, E., Tussiwand, R., Yona, S., 2014. Dendritic cells, monocytes and macrophages: a unified nomenclature based on ontogeny. Nat. Rev. Immunol. 14, 571–578.

Hawiger, D., Inaba, K., Dorsett, Y., Guo, M., Mahnke, K., Rivera, M., Ravetch, J.V., Steinman, R.M., Nussenzweig, M.C., 2001. Dendritic cells induce peripheral T cell unresponsiveness under steady state conditions in vivo. J. Exp. Med. 194, 769–779.

Kaplan, M.H., Schindler, U., Smiley, S.T., Grusby, M.J., 1996. Stat6 is required for mediating responses to IL-4 and for development of Th2 cells. Immunity 4, 313–319.

Kato, Y., Zaid, A., Davey, G.M., Mueller, S.N., Nutt, S.L., Zotos, D., Tarlinton, D.M., Shortman, K., Lahoud, M.H., Heath, W.R., Caminschi, I., 2015. Targeting antigen to Clec9A primes follicular Th cell memory responses capable of robust recall. J. Immunol. 195, 1006–1014.

Krishnaswamy, J.K., Gowthaman, U., Zhang, B., Mattsson, J., Szeponik, L., Liu, D., Wu, R., White, T., Calabro, S., Xu, L., et al., 2017. Migratory CD11b(+) conventional dendritic cells induce T follicular helper cell-dependent antibody responses. Sci Immunol 2.

Laouar, Y., Welte, T., Fu, X.Y., Flavell, R.A., 2003. STAT3 is required for Flt3L-dependent dendritic cell differentiation. Immunity 19, 903–912.

Lewis, S.M., Williams, A., Eisenbarth, S.C., 2019. Structure and function of the immune system in the spleen. Sci Immunol 4.

Leylek, R., Alcantara-Hernandez, M., Lanzar, Z., Ludtke, A., Perez, O.A., Reizis, B., Idoyaga, J., 2019. Integrated cross-species analysis identifies a conserved transitional dendritic cell population. Cell Rep. 29, 3736–3750 e3738.

Li, J., Lu, E., Yi, T., Cyster, J.G., 2016. EBI2 augments Tfh cell fate by promoting interaction with IL-2-quenching dendritic cells. Nature 533, 110–114.

Longhi, M.P., Trumpfheller, C., Idoyaga, J., Caskey, M., Matos, I., Kluger, C., Salazar, A. M., Colonna, M., Steinman, R.M., 2009. Dendritic cells require a systemic type I interferon response to mature and induce CD4+ Th1 immunity with poly IC as adjuvant. J. Exp. Med. 206, 1589–1602.

Lu, E., Dang, E.V., McDonald, J.G., Cyster, J.G., 2017. Distinct oxysterol requirements for positioning naive and activated dendritic cells in the spleen. Sci Immunol 2.

Matheu, M.P., Sen, D., Cahalan, M.D., Parker, I., 2008. Generation of bone marrow derived murine dendritic cells for use in 2-photon imaging. J Vis Exp.

Mebius, R.E., Kraal, G., 2005. Structure and function of the spleen. Nat. Rev. Immunol. 5, 606–616.

Menges, M., Baumeister, T., Rossner, S., Stoitzner, P., Romani, N., Gessner, A., Lutz, M. B., 2005. IL-4 supports the generation of a dendritic cell subset from murine bone marrow with altered endocytosis capacity. J. Leukoc. Biol. 77, 535–543.

Mesin, L., Ersching, J., Victora, G.D., 2016. Germinal center B cell dynamics. Immunity 45, 471–482.

Minty, A., Chalon, P., Derocq, J.M., Dumont, X., Guillemot, J.C., Kaghad, M., Labit, C., Leplatois, P., Liauzun, P., Miloux, B., et al., 1993. Interleukin-13 is a new human lymphokine regulating inflammatory and immune responses. Nature 362, 248–250.

Patente, T.A., Pinho, M.P., Oliveira, A.A., Evangelista, G.C.M., Bergami-Santos, P.C., Barbuto, J.A.M., 2018. Human dendritic cells: their heterogeneity and clinical application potential in cancer immunotherapy. Front. Immunol. 9, 3176.

Pereira, J.P., Kelly, L.M., Xu, Y., Cyster, J.G., 2009. EBI2 mediates B cell segregation between the outer and centre follicle. Nature 460, 1122–1126.

Roco, J.A., Mesin, L., Binder, S.C., Nefzger, C., Gonzalez-Figueroa, P., Canete, P.F., Ellyard, J., Shen, Q., Robert, P.A., Cappello, J., et al., 2019. Class-switch recombination occurs infrequently in germinal centers. Immunity 51, 337–350 e337.

Shin, C., Han, J.A., Choi, B., Cho, Y.K., Do, Y., Ryu, S., 2016. Intrinsic features of the CD8alpha(-) dendritic cell subset in inducing functional T follicular helper cells. Immunol. Lett. 172, 21–28.

Shin, C., Han, J.A., Koh, H., Choi, B., Cho, Y., Jeong, H., Ra, J.S., Sung, P.S., Shin, E.C., Ryu, S., Do, Y., 2015. CD8alpha(-) dendritic cells induce antigen-specific T follicular helper cells generating efficient humoral immune responses. Cell Rep. 11, 1929–1940.

Steinman, R.M., Hemmi, H., 2006. Dendritic cells: translating innate to adaptive immunity. Curr. Top. Microbiol. Immunol. 311, 17–58.

Strioga, M., Schijns, V., Powell Jr., D.J., Pasukoniene, V., Dobrovolskiene, N., Michalek, J., 2013. Dendritic cells and their role in tumor immunosurveillance. Innate Immun. 19, 98–111.

Sulczewski, F.B., Martino, L.A., Almeida, B.D.S., Zaneti, A.B., Ferreira, N.S., Amorim, K., Yamamoto, M.M., Apostolico, J.S., Rosa, D.S., Boscardin, S.B., 2020. Conventional type 1 dendritic cells induce TH 1, TH 1-like follicular helper T cells and regulatory T cells after antigen boost via DEC205 receptor. Eur. J. Immunol.

Trumpfheller, C., Caskey, M., Nchinda, G., Longhi, M.P., Mizenina, O., Huang, Y., Schlesinger, S.J., Colonna, M., Steinman, R.M., 2008. The microbial mimic poly IC induces durable and protective CD4+ T cell immunity together with a dendritic cell targeted vaccine. Proc. Natl. Acad. Sci. U. S. A. 105, 2574–2579.

Turqueti-Neves, A., Otte, M., Prazeres da Costa, O., Hopken, U.E., Lipp, M., Buch, T., Voehringer, D., 2014. B-cell-intrinsic STAT6 signaling controls germinal center formation. Eur. J. Immunol. 44, 2130–2138.

Vento-Tormo, R., Company, C., Rodriguez-Ubreva, J., de la Rica, L., Urquiza, J.M., Javierre, B.M., Sabarinathan, R., Luque, A., Esteller, M., Aran, J.M., et al., 2016. IL-4 orchestrates STAT6-mediated DNA demethylation leading to dendritic cell differentiation. Genome Biol. 17, 4.

Viant, C., Weymar, G.H.J., Escolano, A., Chen, S., Hartweger, H., Cipolla, M., Gazumyan, A., Nussenzweig, M.C., 2020. Antibody affinity shapes the choice between memory and germinal center B cell fates. Cell 183, 1298–1311 e1211.

Yi, T., Cyster, J.G., 2013. EBI2-mediated bridging channel positioning supports splenic dendritic cell homeostasis and particulate antigen capture. Elife 2, e00757.

Yin, X., Chen, S., Eisenbarth, S.C., 2021. Dendritic cell regulation of T helper cells. Annu. Rev. Immunol.

Yousif, A.S., Ronsard, L., Shah, P., Omatsu, T., Sangesland, M., Bracamonte Moreno, T., Lam, E.C., Vrbanac, V.D., Balazs, A.B., Reinecker, H.C., Lingwood, D., 2021. The persistence of interleukin-6 is regulated by a blood buffer system derived from dendritic cells. Immunity 54, 235–246 e235.